Evaluation of numerical models for predicting surface integrity in metal cutting

José Outeiro, Domenico Umbrello, Rachid M'Saoubi, I.S. Jawahir

HAL Id: hal-01064048

https://hal.science/hal-01064048

Submitted on 4 Oct 2017

EVALUATION OF NUMERICAL MODELS FOR PREDICTING SURFACE INTEGRITY IN METAL CUTTING

J.C. Outeiro[1,*], D. Umbrello[2], R. M'Saoubi[3], I. S. Jawahir[4]

[1] LaBoMaP, Arts et Metiers ParisTech,

71250 Cluny, France

[2] Department of Mechanical Engineering, Energy and Management Engineering,

University of Calabria, CS-87036 Rende, Italy

[3] R&D Materials and Technology Development, Seco Tools AB,

SE-73782 Fagersta, Sweden

[4] Institute for Sustainable Manufacturing (ISM),

University of Kentucky, Lexington, KY 40506, USA

ABSTRACT

Efforts on numerical modelling and simulation of metal cutting operations continue to increase due to the growing need for predicting the machining performance. A significant number of numerical methods, especially the Finite Element (FE) and the Mesh-free

---

[*] Corresponding author. Prof. J.C. Outeiro, Arts et Metiers ParisTech, Centre of Cluny, Rue Porte de Paris,

F-71250 Cluny, France. Phone. : +33 3 85 59 53 58. Fax : +33 3 85 59 53 70. E-mail:

jose.OUTEIRO@ensam.eu

methods, are being developed and used to simulate the machining operations. However, the effectiveness of the numerical models to predict the machining performance depends on how accurate are them to represent the actual metal cutting process, and also on the quality and accuracy of the input data used in such models.

This paper presents results from a recently conducted benchmark study, which involved evaluation of various numerical predictive models. This study had a major objective to evaluate the effectiveness of the current numerical predictive models for machining performance, focusing on surface integrity. Five representative work materials were carefully selected for this study from a range of most commonly used work materials, along with a wide range of cutting conditions usually found in the published literature. The differences between the predicted results obtained from several numerical models using different FE and Mesh-free codes are evaluated and compared with those obtained experimentally.

INTRODUCTION AND METHODOLOGY

Modelling and simulation of metal cutting operations have become very popular today with many universities, research institutions and companies developing and/or using various models to predict the machining performance in terms of cutting forces, temperatures, hardness, microstructural and phase changes, residual stresses, tool-wear, part distortion, surface roughness, chip breaking/breakability, process dynamics , stability

of machining operations, etc. (Altintaş and Budak, 1995; Mabrouki et al., 2008; Outeiro et al., 2006b; Umbrello et al., 2007, 2010a; Valiorgue et al., 2007). The effectiveness of these models to predict the machining performance has been questionable due to poor representation of the actual metal cutting process in these models, and the inadequate quality and accuracy of the input data used in such models.

Over the last few decades, analytical and empirical models were most commonly developed and applied to predict mainly cutting forces and temperatures. However, since the early 1980s, the rapidly increased computational capabilities, with the use of computer-based modelling and simulation methods based on Finite Element Method (FEM), have gained a significant application potential. Today, these models have a prominent place in the metal cutting simulation, although it must be stated very clearly that the FEM-based models inherently incorporates many simplistic assumptions that cannot be easily detected by its users, but that affect the validity of the results (Astakhov and Outeiro, 2008).

Within the scope of the recent CIRP (The International Academy for Production Engineering) Collaborative Working Group (CWG) on Surface Integrity and Functional Performance of Components, which operated during 2007-2011, it was decided to conduct a benchmark study to evaluate the effectiveness of all current numerical models for surface integrity induced by metal cutting processes, for predicting not only the most commonly predicted parameters such as cutting forces, temperatures, chip compression ratio and chip geometry, but also parameters related to the integrity/quality of the machined surface, such as residual stresses, hardness and phase transformation (Jawahir et al., 2011). It was hoped

that the results of this benchmark could help the metal cutting researchers to establish future research directions for improved model development.

The methodology adopted in this study involves a careful designing and conducting of a benchmark study for evaluating predictive models for orthogonal cutting, which is composed of the following steps:

1) Selection of the cutting conditions (including the work materials, cutting tools and cutting parameters) and acquiring experimental data for model validation

2) Models development and performing machining simulations for predicting the most significant output parameters, covering the following:

   • General information about the metal cutting models

   • Identification of the work material and cutting tool properties

   • Model calibration

3) Comparison of the results obtained from different models with experimental data, applying two procedures:

   • Without calibration

   • With calibration

This benchmark study was conducted in close cooperation and collaboration with 22 international researchers from 10 countries. The majority of the participants were from Universities or Research Institutes (76%) and the remaining participants were companies and/or software developers (24%).

SELECTION OF CUTTING CONDITIONS AND EXPERIMENTAL DATA ACQUISITION FOR MODEL VALIDATION

In order to test the predictive capability of the numerical simulation models, experimental machining data was acquired for different combinations of cutting tools and work materials. Table 1 summarizes these experimental cutting conditions used in the benchmark work, where the following workpiece materials were considered:

- Plain Carbon Steel, *AISI 1045;*

- Hardened Steel, *AISI 52100;*

- Austenitic Stainless Steel, *AISI 316L;*

- Inconel Alloy, *IN 718;* and

- Titanium Alloy, *Ti-6Al-4V.*

For *AISI 316L, AISI 1045* and *AISI 52100* work materials, the experimental data obtained from orthogonal cutting tests was used from previously published literature (M'Saoubi et al., 1997; Outeiro et al., 2010; Umbrello et al., 2010b), and for *IN718* and *Ti-6Al-4V* work materials, orthogonal cutting experiments using flat-faced uncoated carbide tool inserts were carried out within the framework of the present study. Several parameters were determined, including:

- cutting (F_c) and thrust (F_t) Forces;

- temperature distribution, including cutting temperature (T_c), defined as the maximum temperature at the tool-chip interface;

- Chip Compression Ratio (CCR), defined as the ratio between the uncut chip thickness and the chip thickness;

- chip geometry (peak, valley and pitch); and

- residual stresses in machined surface and subsurface.

Reference	Workmaterial	Tool material	γ (°)	α (°)	r_n (µm)	Rake face Geometry	v_c (m/min)	h_1 (mm)	a_p (mm)
316L-1	AISI 316L (170 Hv)	Uncoated WC-Co	0	5	13	_____	150	0,1	4
316L-2	AISI 316L (170 Hv)	Uncoated WC-Co	5	5	13	_____	150	0,1	4
1045-1	AISI 1045 (200 BHN)	Uncoated WC-Co	-7	7	15	Groove	175	0,05	3
1045-2	AISI 1045 (200 BHN)	Uncoated WC-Co	-7	7	55	Groove	175	0,05	3
52100-1	AISI 5210 (56,5 HRC)	PcBN	-8	8	15	Chamfer (0.10mmx20°)	75	0,125	2,5
52100-2	AISI 5210 (56,5 HRC)	PcBN	-8	8	15	Chamfer (0.10mmx20°)	75	0,125	2,5
718-1	IN 718 (42 HRC, annealed +Aged)	Uncoated WC-Co	6	7	30	_____	55	0,15	4
718-2	IN 718 (42 HRC, annealed +Aged)	Uncoated WC-Co	6	7	30	_____	90	0,15	4
Ti-1	Ti-6Al-4V (35 HRC)	Uncoated WC-Co	6	7	30	_____	55	0,15	4
Ti-2	Ti-6Al-4V (35 HRC)	Uncoated WC-Co	6	7	30	_____	90	0,15	4

Table 1 Cutting conditions used in the benchmark study (Jawahir et al., 2011).

MODEL DEVELOPMENT AND SIMULATION OF PREDICTIVE

PERFORMANCE OF MOST SIGNIFICANT OUTPUT PARAMETERS

General Information About the Metal Cutting Models and Software

The simulations were performed using commercial and non-commercial software programs/packages, at given percentage of utilisation: Deform (47%), Abaqus (30%), Advantedge (10%), LS-Dyna (10%), and a non-commercial software package developed at Yokohama National University (10%). The main features of these software packages to simulate the metal cutting process will be explained below, and this includes: (i) Finite Element (FE) and Mesh-less methods (ii) Lagragian and Arbitrary Lagrangian-Eulerian (ALE) formulations; (iii) implicit and explicit time integration algorithms; (iv) constitutive and damage models; and (v) friction models. A general description about these features can be found in a previous work (Astakhov and Outeiro, 2008).

Deform uses a Lagrangian formulation together with implicit time integration to simulate both two- and three-dimensional metal cutting processes, including turning, milling and drilling. This software has a relatively better user-friendly interface to set-up the model (Pre-Processor) and to analyse the results of the simulations (Post-Processor). Several constitutive models are embedded in the graphical interface, including the well known Johnson-Cook constitutive model. Other models can be implemented in the software by developing simple subroutines. The chip formation process is modelled using a remeshing procedure, where the chip is formed due to continuous indentation of the tool in the

workpiece, and by applying a frequent remeshing procedure to minimize the penetration of the tool in the workpiece's mesh. The frequency of the remeshing procedure must be as low as possible, in order to: (i) avoid rapid mesh distortion problems; and (ii) minimize the interpolation errors when transferring the state variables (stress, strain, strain-rate, temperature, etc.) from the previous (distorted) mesh to the current mesh (remapping). The frequency of the remeshing procedure can be adjusted in a function of the maximum allowable penetration depth of the tool in the workpiece's mesh. Several damage models are embedded in the graphical interface (Cockcroft–Latham, Rice and Tracey, etc) (Cockroft and Latham, 1968; Rice and Tracey, 1969), which can be used to model chip segmentation in plastic regime only. As for the constitutive models, other damage models can be implemented in the software by developing simple relevant subroutines. Unfortunately, due to the remeshing procedure, these damage models cannot be used to model chip formation as a fracture process. Deform has two friction models embedded in the graphical interface, the Coulomb and shear friction models, while other models can be implemented in the software by developing simple subroutines.

Abaqus uses both Lagrangian, and Arbitrary Lagrangian-Eulerian (ALE) formulations together with implicit and explicit time integrations to simulate both two- and three-dimensional metal cutting processes, including turning, milling and drilling. The Abaqus CAE user interface is accessible, although more difficult to use than Deform's user interface. Similar to Deform, Abaqus comes with several constitutive and damage models embedded in its graphical interface, including the Johnson-Cook models. Also, both Coulomb and shear friction models are embedded in the graphical interface. Similar to

8

Deform, other constitutive/damage/friction models can be implemented in Abaqus by developing a subroutine. The main advantage of Abaqus when compared to Deform is that several numerical procedures can be used to model the chip formation process.

Associated with the Lagrangian formulation, the material separation from the workpiece to generate the chip formation process can be accurately described by a fracture process, which can be modelled numerically using element deletion or node splitting techniques. The separation occurs along a pre-defined path, when a given geometric or physic criterion is satisfied, such as shown in (Huang and Black, 1996): (i) the distance between the tool tip and the workpiece's node immediately ahead is equal to or less than a critical distance; (ii) the stress/strain/energy in the workpiece´s node/element immediately ahead of the tool is equal to or greater than a critical value. Rather than the criterion used to produce chip formation, the proper determination of the critical value is the key issue (Huang and Black, 1996). In the case of a physics-based criterion such as the critical strain, several mechanical tests are required to determine the fracture strain under different stress triaxility, strain-rates and temperatures (Abushawashi et al., 2011; Mabrouki et al., 2008). Although the drawbacks associated with the Lagrangian formulation involves the elements distortion and due to the fact that the separation path is not known a priori, particularly when chamfered and/or negative rake or heavy-radii cutting edge tools are involved in the simulation (Movahhedy et al., 2000), this approaches can model with good accuracy the chip formation process for high ratios of uncut chip thickness to cutting edge radius (high tool sharpness).

Associated with the ALE formulation, the chip formation is usually modelled to simulate the material flow around the cutting edge. The ALE formulation has two major drawbacks.

ALE formulation cannot prevent the need for a re-meshing procedure and consequently remapping of state variables. Moreover, no physical separation occurs in generating the chip, which is inadequate to simulate the chip formation, in particular in brittle materials where this separation is caused by a fracture process.

AdvantEdge uses a Lagrangian formulation together with explicit time integration to simulate both two- and three-dimensional metal cutting processes, including turning, milling and drilling. This software has a very user-friendly interface to set-up the model (Pre-Processor) and to analyse the results of the simulations (Post-Processor). Several constitutive and friction models are embedded in the graphical interface. Unfortunately, the implementation of other constitutive and friction models is not accessible by the users. Moreover, the chip formation is modelled in the same way as Deform, thus suffering from the same drawbacks.

LS-Dyna uses both Lagrangian and Arbitrary Lagrangian-Eulerian (ALE) formulations together with implicit and explicit time integrations to simulate both two- and three-dimensional metal cutting processes. In this study, this software was exclusively used to perform the orthogonal cutting simulations by applying the mesh-less method, namely the Smooth Particle Hydrodynamics (SPH) Lagrangian method. This method is also available in the most recent versions of Abaqus. The main advantage of the mesh-less methods when compared with the FE based methods is the inexistence of elements distortion, since the model is defined by a number of mesh-points (particles) instead of a mesh. Therefore, large strains are easily handled, as it is the case of the metal cutting process. LS-Dyna has

also an accessible interface, although more difficult to use than the others software's user interface. It comes also with several constitutive, damage and friction models embedded in its graphical interface, including the Johnson-Cook constitutive/damage models. Also, other constitutive/damage/friction models can be implemented in LS-Dyna by developing special subroutines. As well as in Abaqus, several numerical procedures can also be used to model the chip formation process.

Table 2 summarizes the major features of these three commercial software packages. In the present benchmark study, the different participants and collaborators used all of the above-mentioned features. Moreover, all the simulations were performed under plane-strain conditions and by applying coupled thermo-mechanical analysis.

	Deform	Abaqus	Ls-Dyna	Advantedge
Formulation	Lagrangian; ALE	Lagrangian; Eulerian; ALE	Lagrangian; Eulerian; ALE	Lagrangian
Algorithm of time integration	Implicit	Implicit; Explicit	Implicit; Explicit	Explicit
Constitutive models	Elasto-visco-plastic: • Jonhson-Cook • Other models • User routine	Elasto-visco-plastic: • Jonhson-Cook • Other models • User routine	Elasto-visco-plastic: • Jonhson-Cook • Other models • User routine	Elasto-visco-plastic: • Jonhson-Cook • Other models
Damage models	• Cockcroft–Latham • Brozzo • Other models • User routine	• Jonhson-Cook • Other models • User routine	• Jonhson-Cook • Other models • User routine	
Chip formation techniques	• Continuous tool indentation and remehing	• Node-splitting • Element deletion • No separation	• Node-splitting • Element deletion • No separation	Continuous tool indentation and remehing
Chip segmentation ?	Only in plastic	yes	yes	yes
Friction	• Coulomb friction • Shear friction • User routine	• Coulomb friction • Shear friction • User routine	• Coulomb friction • Shear friction • User routine	Coulomb
Analysis	Coupled thermo-mechanical			

Table 2 Major features of the commercial FEM software packages used for metal cutting simulation

Identification of the Work Material and Cutting Tool Properties

In order to reproduce a common practice used in most scientific publications dealing with modelling of metal cutting operations, the work material properties used in this benchmark study were picked up from several bibliographical references. Table 6 summarize the mechanical and thermo-physical properties of the different work materials and cutting tools used in this study. The Poisson ratio (V) and Young's modulus were used to model the elastic behaviour of the selected five work materials. To model the thermo-viscoplastic

behaviour of *AISI 1045, AISI 316L, IN718* and *Ti6Al4V* work materials, a Johnson-Cook's constitutive equation (Johnson and Cook, 1983) was employed, as follows:

$$\sigma = \left(A + B\varepsilon^n\right)\left[1 + C\ln\left(\frac{\dot{\varepsilon}}{\dot{\varepsilon}_0}\right)\right]\left[1 - \left(\frac{T - T_{room}}{T_m - T_{room}}\right)^m\right] \tag{1}$$

where ε is the plastic strain, $\dot{\varepsilon}$ is the strain-rate (s^{-1}), $\dot{\varepsilon}_0$ is the reference plastic strain-rate, T (°C) is the workpiece temperature, T_m is the melting temperature of the work material and T_{room} (20°C) is the room temperature. Coefficient A (MPa) is the yield strength, B (MPa) is the hardening modulus, C is the strain-rate sensitivity coefficient, n is the hardening coefficient and m the thermal softening coefficient. The values of these coefficients were obtained from the literature and are shown in Table 3.

Regarding the *AISI 52100* work material, a hardness-based flow stress model was developed by Umbrello et al. (Johnson and Cook, 1983; Umbrello et al., 2010b). Similar to the Johnson-Cook constitutive model, this mew model also takes into account the effects of the strain, effective strain-rate, temperature, and in additional the hardness on the flow stress. This model is formulated as follows:

$$\sigma\left(\varepsilon, \dot{\varepsilon}, T, HRc\right) = B\left(T\right)\left(C\varepsilon^n + J + K\varepsilon\right)\left[1 + \left(\ln\left(\dot{\varepsilon}\right)^m - A\right)\right] \tag{2}$$

where B is a temperature-dependent coefficient, C represents the work hardening coefficient, J and K are two linear functions of hardness, A is a constant. The detailed explanation of the terms in the above equation can be found in (Johnson and Cook, 1983).

Workmaterial	A (MPa)	B (MPa)	C	n	m	$\dot{\varepsilon}_0$ (s^{-1})	Tmelt (°C)
AISI 316L	305	1161	0,010	0,610	0,517	1	1400
AISI 1045	553	601	0,0134	0,234	1	1	1460
IN718	980	1370	0,020	0,164	1,03	1	1300
Ti6Al4V	1098	1092	0,014	0,93	1,1	1	1660
AISI 52100	See bibliographic references						

Table 3 Coefficients of the constitutive models of the workmaterials.

Workmaterial	Tool material	ρ (Kg/m^3)	E (GPa)	v
AISI 316L	WC-Co	14950	613	0,22
AISI 1045	WC-Co	13000	650	0,15
AISI 52100	PcBN	4084	800	0,15
IN718	WC-Co	14933	660	0,22
Ti6Al4V	WC-Co	14933	660	0,22

Table 4 Elastic properties of the tool materials.

Workmaterial	ρ (Kg/m³)		E (GPa)		ν		α (m/m °C)	
	T (°C)	ρ	T (°C)	E	T (°C)	ν	T (°C)	α x10^{-5}
AISI 316L	0 100 200 400 600 800 1000	7900 7900 7800 7700 7600 7600 7500	20 100 200 400 600 800	196 192 185 169 151 132	20 100 200 400 600 800	0,26 0,26 0,27 0,3 0,28 0,27	200 400 600 800 1000	1,65 1,75 1,85 1,9 1,95
AISI 1045	20 200 400 600 800	7930 7880 7820 7750 7720	0 20 100 200 300 400 500 600	213 212 207 199 192 184 175 164	0,29		0 20 100 200 300 400 500 600	1,17 1,19 1,25 1,3 1,36 1,41 1,45 1,49
IN718	8190		20 871	217 156	0,3		20 250 500	1,22 1,38 1,44
Ti6Al4V	See bibliographic references							
AISI 52100	7810		20 200 400 600 800 1000	201 179 163 103 87 67	20 200 400 600 800 1000	0.28 0.27 0.26 0.34 0.39 0.49	20 100 200 300 400 500 600	1.19 1.25 1.30 1.36 1.41 1.45 1.49

Table 5 Elastic properties of the work materials.

Workmaterial	Tool material	Workmaterial				Tool material			
		λ (W·m^{-1}·K^{-1})		c_p (J·Kg^{-1}·K^{-1})		λ (W·m^{-1}·K^{-1})		c_p (J·Kg^{-1}·K^{-1})	
		T (°C)	λ	T (°C)	c_p	T (°C)	λ	T (°C)	c_p
AISI 316L	WC-Co	20 200 400 500 600 800	14,6 17,9 20,5 21,7 23,4 25,1	20 200 400 600 800 1000	452 523 561 582 628 722	72,5		138	
AISI 1045	WC-Co	20 100 200 300 400 500 600	41,7 43,4 43,2 41,4 39,1 36,7 34,1	20 100 200 300 400 500 600	461 496 533 568 611 677 778	62,7		234	
AISI 52100	PcBN	20 100 200 300 400 500 600 700 800 1000 1200	52.5 50.7 48.1 45.7 41.7 38.3 33.9 30.1 24.8 32.9 29.8	20 100 200 250 300 350 400 500 600 700 750 800 900	474 488 517 530 401 572 589 652 711 773 1589 626 551	40		558	
IN718	WC-Co	20 100 200 300 400 500 600 700 800 900 1000 1100 1200	10,3 11,9 13,6 15,2 16,7 18,5 20,9 24,1 26,1 25,7 26,3 29,0 31,0	20 100 200 300 400 500 600 700 800 900 1000 1100 1200	442 461 477 489 503 523 562 613 664 653 675 695 713	0 200 400 600 800 1000 1200	129,3 101,7 77,4 65,0 58,0 53,5 49,5	0 90 200 400 600 800 940 970 1000 1200	196 220 235 256 271 287 302 293 292 295
Ti6Al4V	WC-Co	See bibliographic references				0 200 400 600 800 1000 1200	129,3 101,7 77,4 65,0 58,0 53,5 49,5	0 90 200 400 600 800 940 970 1000 1200	196 220 235 256 271 287 302 293 292 295

Table 6 Thermal properties of the work and tool materials.

Models' Calibration

In order to improve the metal cutting models, a calibration procedure is frequently used. This poses difficulty for the predictability of the model, since to develop a model of a given phenomenon, some experimental data related to this phenomenon is required.

The common calibration process of the numerical model for machining operation is shown in Figure 1. In particular, for this benchmark study, the models and the relative values of the friction coefficients were determined through an iterative calibration process using the experimental data on cutting forces. Different damage and failure models or numerical approaches related to simulation of serrated chips, using a modified material flow stress model incorporating "flow softening" effects, were chosen, and calibrated by comparing the chip morphology. Finally, the heat transfer coefficient h_{int} at the tool-chip-work interfaces was found through an iterative calibration process using the experimental data from the temperature fields of tool-workpiece-contact interfaces.

Methodology for Calculating the Residual Stresses and for Extracting Them From the FE Model

The calculation of the predicted residual stresses and their comparison with those measured experimentally has any meaning only when the predicted residual stresses are simulated and extracted from the FE model under the same conditions as those applied experimentally. These conditions will not only depend on the cutting procedure, but also

on the experimental technique and procedure used to measure the residual stresses (Outeiro et al., 2006a).
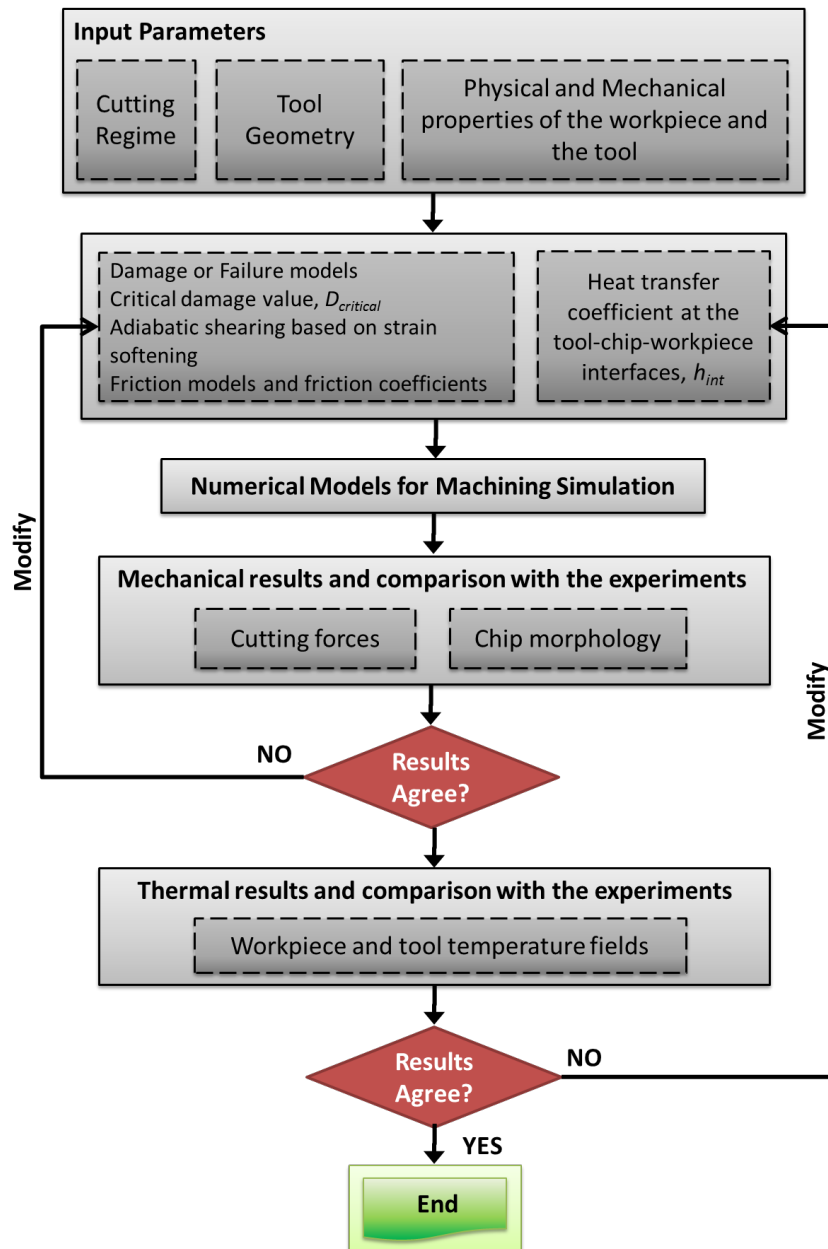

Figure 1 Flow chart for the calibration of the numerical models for machining simulation.

The following methodology should be adopted for calculating the residual stresses and for extracting them from the FE model:

1. Perform metal cutting simulation with at least two cutting passes using a tool geometry with measured flank wear;

2. Calculate the residual stresses;

4. Extract the residual stress components from the FE model.

Perform metal cutting simulation with at least two cutting passes using a tool geometry with measured flank wear

Few studies are reporting variations in the in-depth residual stress profiles from one cut to another (Guo and Liu, 2002; Outeiro et al., 13). Furthermore, the residual stress distributions developed in the previous pass must be considered when simulating the next pass, because experimentally the residual stresses are normally measured after performing several passes.

As far as tool-wear is concerned, it should be monitored during the machining tests and it must be taken into account when modelling the residual stresses. Because, tool-wear influences the cutting process, the residual stresses will be affected (Liu et al., 2004; Marques et al., 2006; Outeiro et al., 13). As a consequence, the residual stresses must be simulated by considering the measured tool-wear.

Calculate the residual stresses

The procedure for calculating the residual stresses may depend on the level of knowledge of the researcher about the residual stresses and of a particular software package, but in any case should include the workpiece's mechanical unloading and cooling down to room

temperature. This procedure can be automatic as is the case of AdvantEdge, or requires the development of an additional model for unloading and cooling down the workpiece. This is the case of the others software packages (Abaqus, Deform and LS-Dyna).

Extracting the predicted residual stress from the FE model

As explained by Outeiro et al. (Outeiro et al., 2006a), if at the end of the simulation the chip is attached to the workpiece, the predicted residual stress components should be extracted from the model sufficiently far away from the chip formation zone. As shown in Figure 2, a strong residual stresses variation is observed near the chip formation zone, which is not representative of the real residual stresses left in the workpiece. In order to avoid this zone, Region III should be selected to evaluate the residual stress components, being its distance from chip root a function of the cutting conditions (cutting speed, feed, depth of cut, tool geometry/material, workpiece material, etc.).
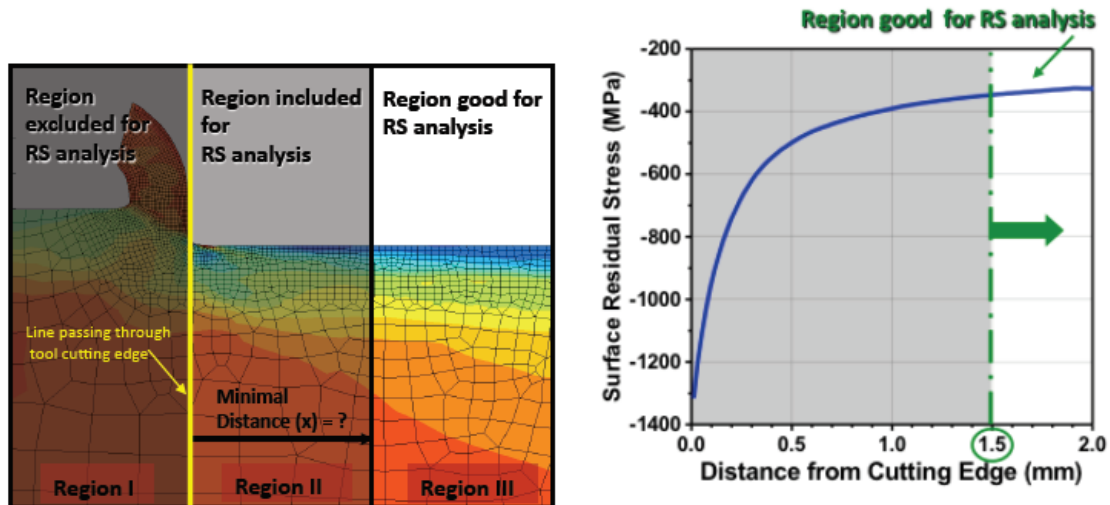
Figure 2. Procedure to extract the residual stress components from the model [18].

In order to compare both predicted and XDR-measured in-depth residual stress profiles, the predicted values need to be weighted using a function that takes into account the absorption of the X-ray in the material under analysis, which can be calculated by the following equation:

$$\left\langle \sigma_R \right\rangle = \frac{\int\limits_{0}^{\infty} \sigma(z) \cdot e^{-z/\tau} dz}{\int\limits_{0}^{\infty} e^{-z/\tau} dz} \tag{3}$$

where τ is the mean penetration depth of the X-ray beam in the material (Outeiro et al., 2013). Also, several residual stress profiles should be extracted from the workpiece, covering a length equal to the length/diameter of the irradiated area in the machined surface. Then, an average residual stress value can be calculated for each depth.

COMPARISON OF THE RESULTS OBTAINED FROM DIFFERENT MODELS WITH EXPERIMENTAL DATA

Without the Calibration Procedure

Figures 3-7 show the measured (black bar) and simulated (color bar) results, for forces (Figure 3 and 4), cutting temperatures, which by definition is the maximum temperature at the tool-chip interface (Figure 1), chip compression ratio (Figure 6) and surface residual stress, σ//, (Figure 7).

Figure 3 shows the predicted and measured cutting force for different work materials and simulation/test conditions. This figure also shows a higher dispersion of simulated cutting force for the case of the *AISI 316L, IN 718* and *Ti6AL4V* work materials and lower for the case of *AISI 1045* and *AISI 52100* work materials. As for the thrust force (Figure 4), except for the *AISI 1045 steel,* all the other work materials exhibit high dispersion. The differences in the cutting and thrust forces are greater than 90% for the cases of *AISI 316L, AISI 52100, IN 718* and *Ti6AL4V*. However, for *AISI 1045* steel, although the differences in the simulated cutting and thrust forces are lower when compared to other work materials, the differences are almost about 50%. As for the comparison between measured and simulated cutting and thrust forces, the best predictions were obtained for the *AISI 1045*.

Figure 5 shows the predicted and measured cutting temperatures for different work materials and simulation/test conditions. This figure shows a high dispersion between predicted cutting temperatures, and this dispersion is higher for *AISI 316L, IN 718* and *Ti6AL4V,* and lower for *AISI 1045*. These results confirm what was previously observed for the cutting and thrust forces, although the differences between the predicted cutting temperatures are lower when compared to the forces. These differences can reach 70-80% for *AISI 316L, IN 718* and *Ti6AL4V* work materials, and a maximum of 30% for the *AISI 1045*. As for the comparison between measured and simulated cutting temperatures, the best predictions were obtained again for *AISI 1045*. It should be pointed out that since no experimental data on cutting temperatures was available for the AISI 52100 work material.

Figure 6 shows the predicted and measured chip compression ratio (CCR) for different work materials and simulation/test conditions. This figure also shows a high dispersion

work materials when compared to the other work materials. The differences in the CCR can reach 70% for the case of *AISI 316L* and *Ti6AL4V,* and are slightly lower (about 50%) for the other work materials. As for the comparison between measured and simulated CCR, the best predictions were obtained for *AISI 52100,* and no experimental data was available for the *AISI 1045* and *AISI 316L* work materials.

Residual stresses were measured in both cutting direction ($\sigma//$) and normal to this direction ($\sigma\perp$), but only the first stress component is presented in this manuscript, because it is the most critical one for the part's functional performance and life in service. Figure 7 shows the predicted and measured surface residual stress, $\sigma//$, for different work materials and simulation/test conditions. This figure shows a higher dispersion of simulated surface residual stress, $\sigma//$, for all work materials, lower for *AISI 52100, AISI 1045* and *AISI 316L* work materials, and higher for the other work materials. In all cases, the differences between the predicted results are greater than 100%, being about 100%-140% for the *AISI 52100, AISI 1045* and *AISI 316L* work materials, and more than 250% for the other work materials. A significant difference between measured and simulated surface residual stress, $\sigma//$, is also observed, being the best predictions obtained for the *AISI 1045* and *AISI 52100* steels. Looking into more details, the in-depth residual stress profiles (Figures 9-13), it appears that this dispersion between simulated residual stresses is once again lower for the *AISI 1045* and higher for *AISI 316L* and *IN 718* work materials. The best fits between measured and simulated residual stresses were obtained for *AISI 1045,* and partially for *AISI 52100* and *Ti-6Al-4V* work materials.

In summary, in general the results show a significant dispersion between simulated results. As shown in Figure 8, the smallest coefficient of variation, which is a normalized measure

of dispersion of a distribution, is observed for the chip compression ratio, while the largest for surface residual stress, σ//. Moreover, the smallest dispersion was obtained for *AISI 1045* and AISI 52100 steels while the largest for *AISI 316L*, *IN 718* and *Ti6Al4V* alloys. As far as the differences between measured and simulated results is concerned, they are also significant, being lower for *AISI 1045,* and in some cases for *AISI 52100* and *Ti-6Al-4V* work materials. The worst predictions were obtained for *AISI 316L* and *IN 718* work materials. The high dispersion between simulated results and their deviation in relation to the experimental results can be mainly attributed to different factors that the participants were free to setup on their own in their simulations. These are:

i) Numerical methods (FEM, Meshless), formulations (Lagrangian, ALE) and corresponding parameters (element size, time step,…) and assumptions: A numerical model incorporates many numerical issues that are not easy to setup by someone who does not have sufficient knowledge about numerical methods. This is particular evident for the software packages Abaqus, LS-Dyna, and to some extent, even Deform. For example, a simple selection of the element size can strongly influence the model's predictions. Moreover, any software package incorporates many assumptions that are not accessible by the users, but strongly affects the model's predictions.

ii) Boundary conditions (thermal and mechanical): The size of the geometrical model of the workpiece and tool, and how the thermal and mechanical boundary conditions are applied to this model can influence the temperature, stress and strains distributions, thus affecting the model's predictive capability.

iii) Procedures for calculating the residual stresses and for extracting them from the model: There is no standard procedure to calculate and extract the residual from the

24

model, and unfortunately, most of the scientific publications do not describe how they have done such calculations and extractions.

iv) Tool-chip and tool-work contact models and parameters (friction coefficient, friction factor, heat transfer coefficient, etc.): The participants were free to select the contact models and the corresponding values of the model's coefficients. The friction coefficient is the most used parameter to describe the relationship between normal and contact stresses. As shown by in previous publications (Astakhov, 2006; Özel and Ulutan, 2012; Rech et al., 2013), this coefficient is not constant along the tool-chip contact, and it depends on the contact conditions (contact pressure, sliding velocity and temperature). An incorrect determination/selection of the friction coefficient can strongly influence/affect the model's predictions.

v) Incorrect description of the mechanical behavior of the work material in machining also contributes to these differences. In particular, the incorrect description of the work material flow stress and fracture in machining. Due to the high importance of this subject, this will be described in detail as follows.

As shown by Astakhov (Astakhov and Shvets, 2004), the principal difference that exists between machining and all other metal forming processes is the physical separation of the layer being removed (in the form of chips) from the rest of the workpiece. The process of physical separation of a solid body into two or more parts is known as fracture, and thus machining must be treated as the purposeful fracture of the layer being removed. From this context, a proper modeling of work material in machining should take into account not only the determination of the material flow stress under similar conditions as those

observed in machining, but also under which conditions the fracture would occurs and how to model it properly.

As far as the flow stress is concerned, the split Hopkinson pressure bar (SHPB) (Kolsky, 1949) is largely used to determine the work material flow stress under high strain-rates frequently encountered to metal cutting. Unfortunately, the SHPB has some drawbacks that can compromise the validity of the results, including the oscillations that flow stress exhibits particularly at low strains (Jaspers, 1999). Moreover, the flow stress depends on the strain path (Guo et al., 2005), which according to Silva et al. (Silva et al., 2012), the strain path induced by the SHPB is different from that found in metal cutting. Finally, the flow stress data is usually represented by the Johnson-Cook (JC) constitutive model (Johnson and Cook, 1983), available in most of the commercial FE codes, including those used in this benchmark study. As mentioned by Guo and Horstemeyer (Guo et al., 2005), although this model is easy to apply and can describe the general response of material deformation, this model is deficient in the mechanisms to reflect the static and dynamic recovery, and the effects of load path and strain-rate history in large deformation processes, such is the case of metal cutting process. These effects are fundamental to proper modeling the surface integrity of machined components, including the residual stress distribution (Guo et al., 2005). Moreover, presuming that no external heat source is added to the cutting process, the term on thermal softening of the JC constitutive model (see Eq. 1) is not necessary. In fact, the heat generated under high strain-rates accelerates the temperature rise and creates adiabatic localized regions in both mechanical tests for the characterization of the material flow stress and machining alike. Thus, the strain-

hardening measured in high rate material testing may have included the thermal softening effects as well (Abushawashi et al., 2011).

As far as damage or fracture is concerned, they are essential to model chip formation (separation of the material from the workpiece to form the chip) as well as for chip segmentation. Therefore, a proper modeling of damage and fracture is essential and the corresponding models should consider both damage initiation, as well as damage evolution (Abushawashi et al., 2011; Mabrouki et al., 2008). In ductile materials, the damage initiation model should be established based on the material ductility, thus the equivalent strain at fracture. The equivalent strain at fracture is sensitive to the state of stress, being the stress triaxility and the Lode angle two parameters that affect this strain (Abushawashi et al., 2013; Bai and Wierzbicki, 2008). In the case of plane-strain condition, which is the case for orthogonal cutting, the equivalent strain at facture is only affected by the stress triaxility (Abushawashi et al., 2011). Increasing exigencies in terms of productivity leads to the application of high cutting speeds (High Speed Machining), and consequently the work material is submitted to high strain-rates. Therefore, the strain-rate sensitivity to fracture must be also included in the fracture model as well. Concerning the temperature effects on the strain at fracture, what was mentioned above is also applied here. Therefore, a suitable model of damage initiation in orthogonal metal cutting should consider both stress triaxility and strain-rate effects. There are several fracture models that incorporate these effects, including the Johnson and Cook (Johnson and Cook, 1983) model and the Rice and Tracey (Rice and Tracey, 1969) fracture models. The determination of the coefficients of these fracture models for a give work material requires resources and involves a series of experimental fracture tests (varying the stress triaxility and strain-rate).

Moreover, the implementation of such models in some FE codes can be a little more complex. For these reasons, in many metal cutting models, the fracture is ignored, because it is easier to model chip formation using non-physical criterion such as the remesh procedure.

To conclude, modeling chip formation without a proper material model, that includes damage and fracture, results in unrealistic material behavior, where the material flow is somewhat unlimited with no material stiffness degradation. Moreover, the chip morphology (e.g., segmentation) obtained by such incomplete models produces an unrealistic smooth chip with unlimited material stretching and hardening (Abushawashi et al., 2013).

Applying the Calibration Procedure

The calibration procedure was applied to four additional orthogonal cutting simulations performed on *IN 718* and *Ti-6Al-4V* alloys (two simulations peer work material). The objective is to develop and calibrate new models based on the measured forces, chip geometry and chip compression ratio, and apply them to predict the residual stresses. Figure 14 and 15 show that although a small improvement was seen in the near surface residual stress for *Ti-6Al-4V,* no other relevant improvement was observed.

These results prove that the calibration procedure was not able to improve the model's "predictability" and a very important part of the solution for the problem is to consider a proper material model that includes not only flow stress, but also damage and fracture.
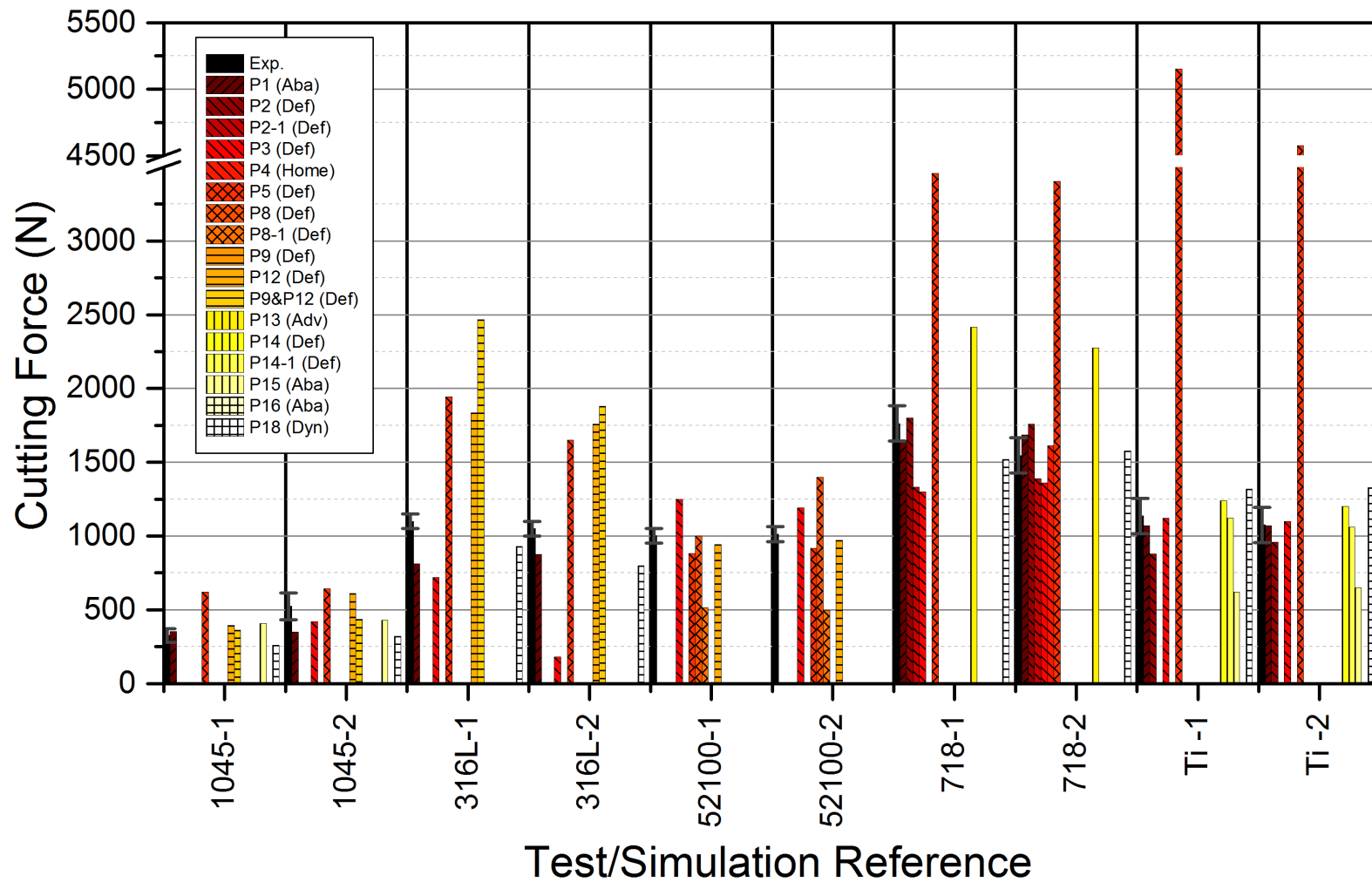
Figure 3. Simulated (color bars) and measured (black bar) cutting force values for different work materials and cutting conditions.
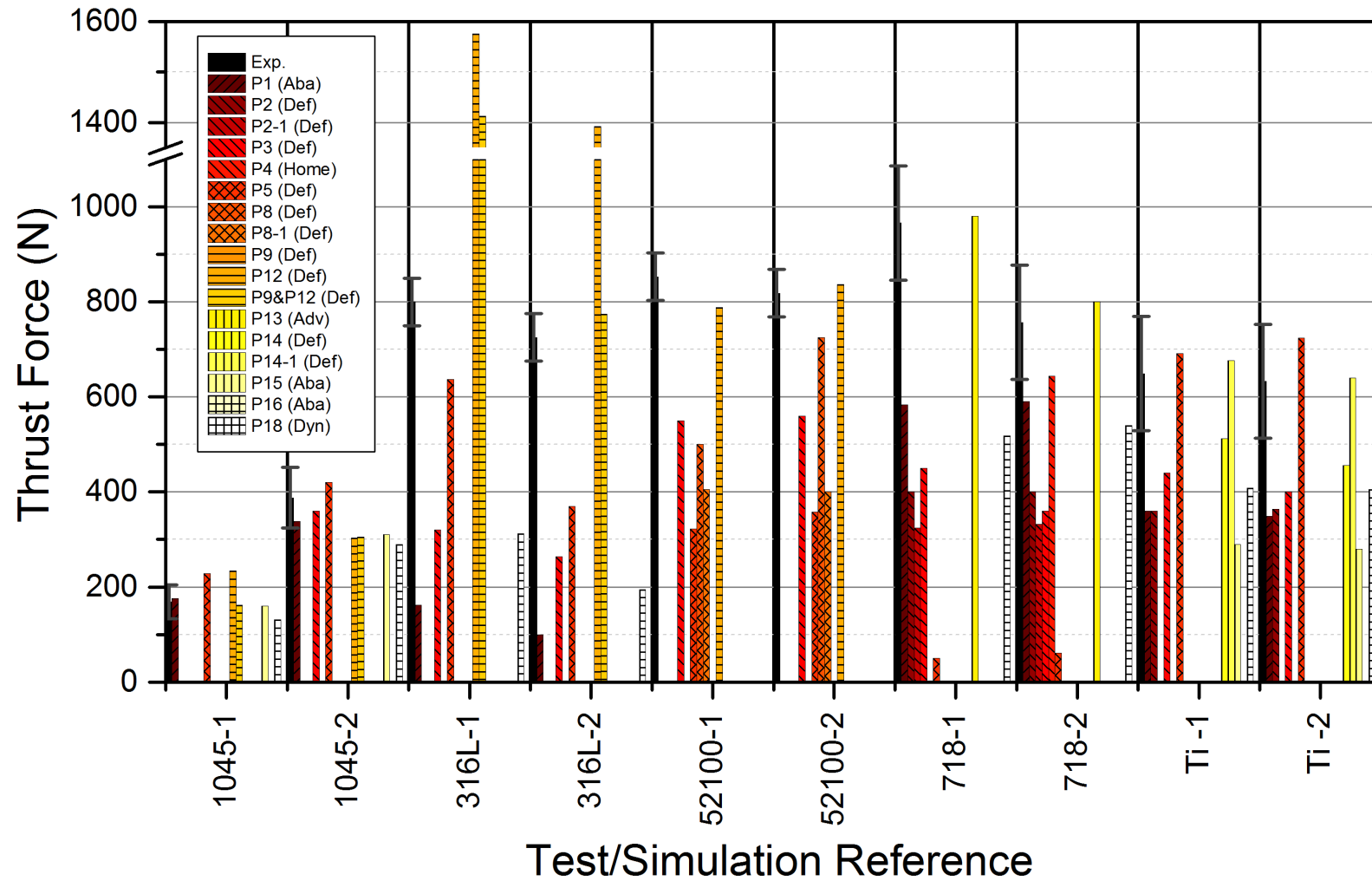
Figure 4. Simulated (color bars) and measured (black bar) thrust force values for different work materials and cutting conditions.
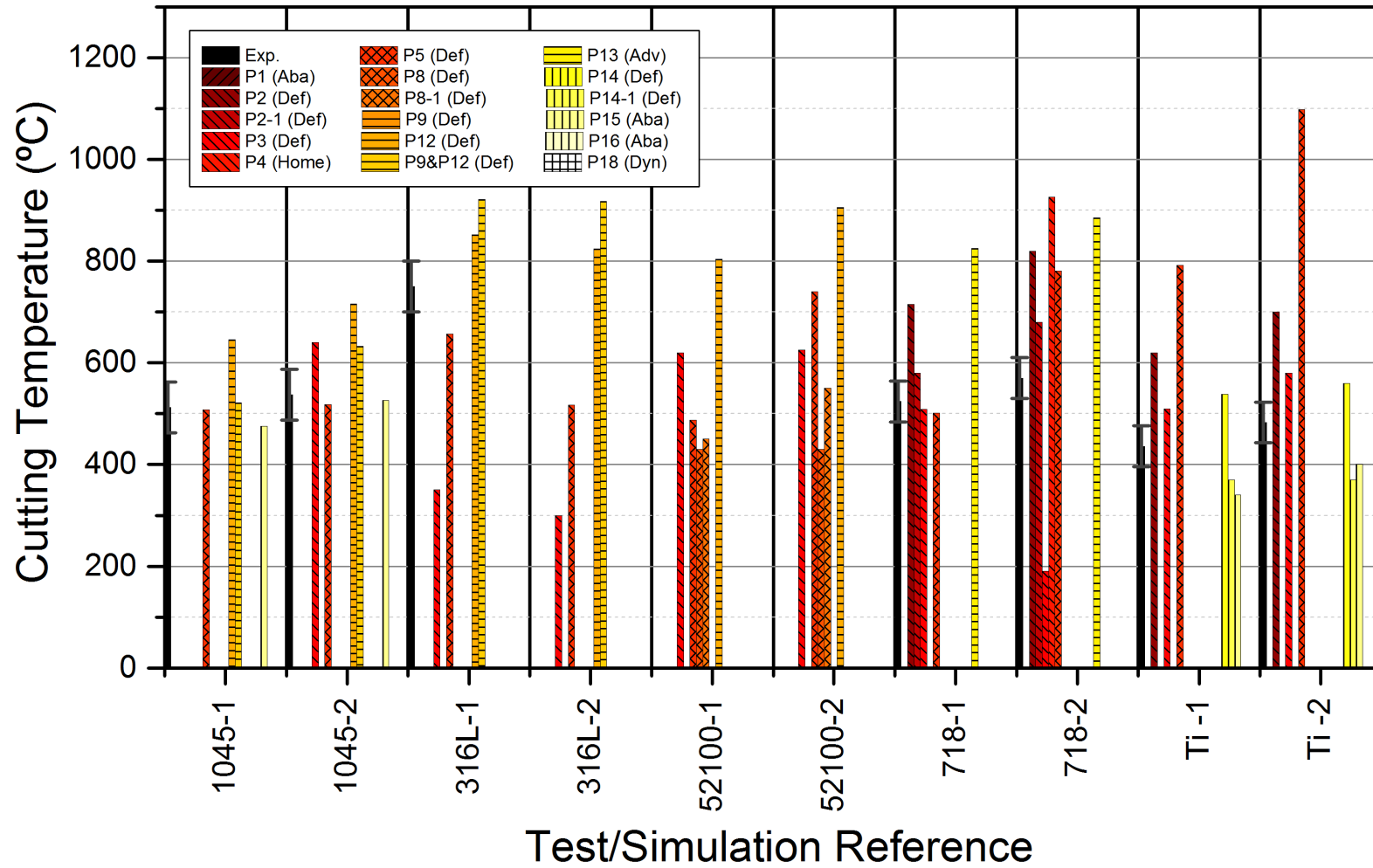
Figure 5. Simulated (color bars) and measured (black bars) cutting temperatures (the maximum temperature at the tool-chip interface) for different work materials and cutting conditions
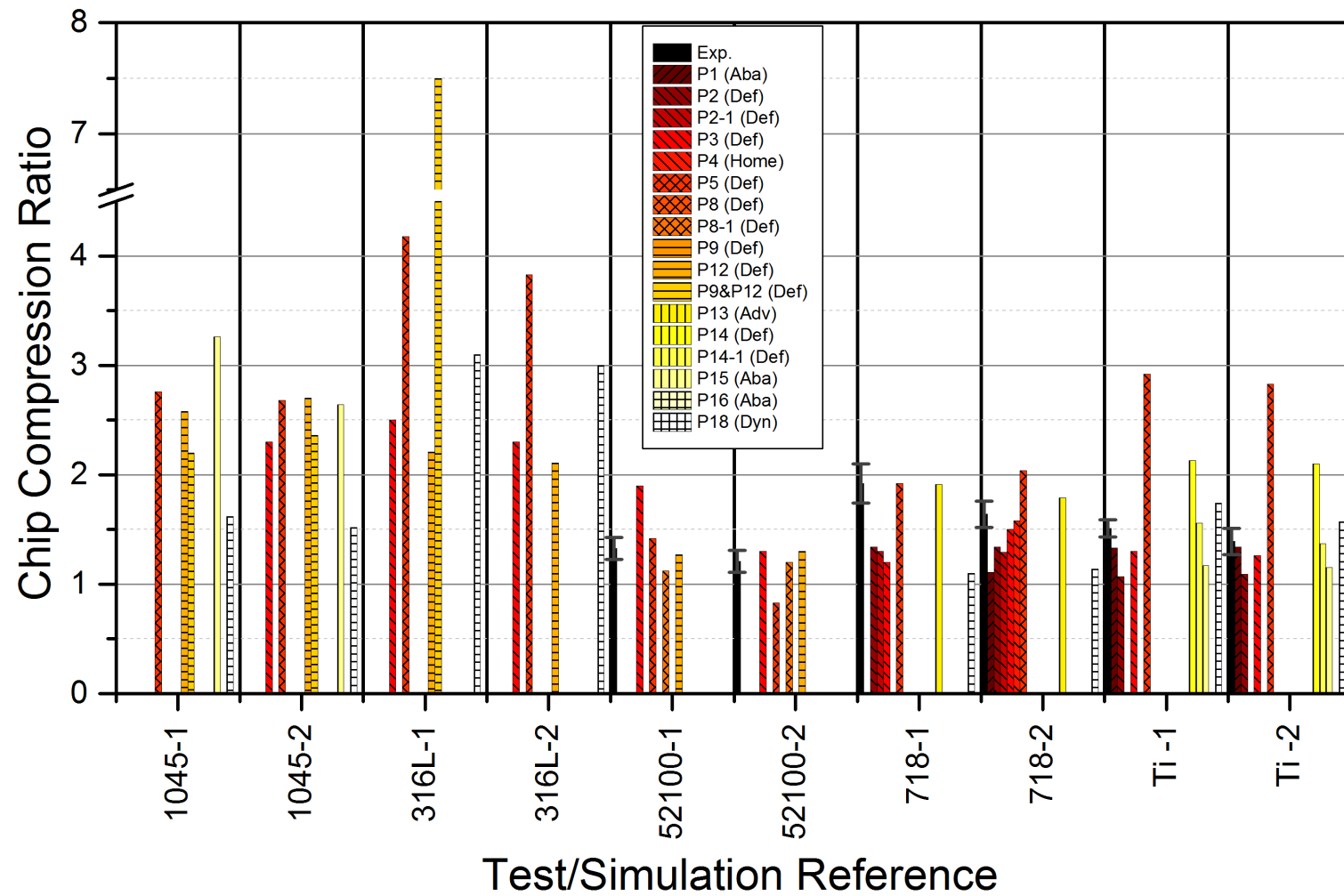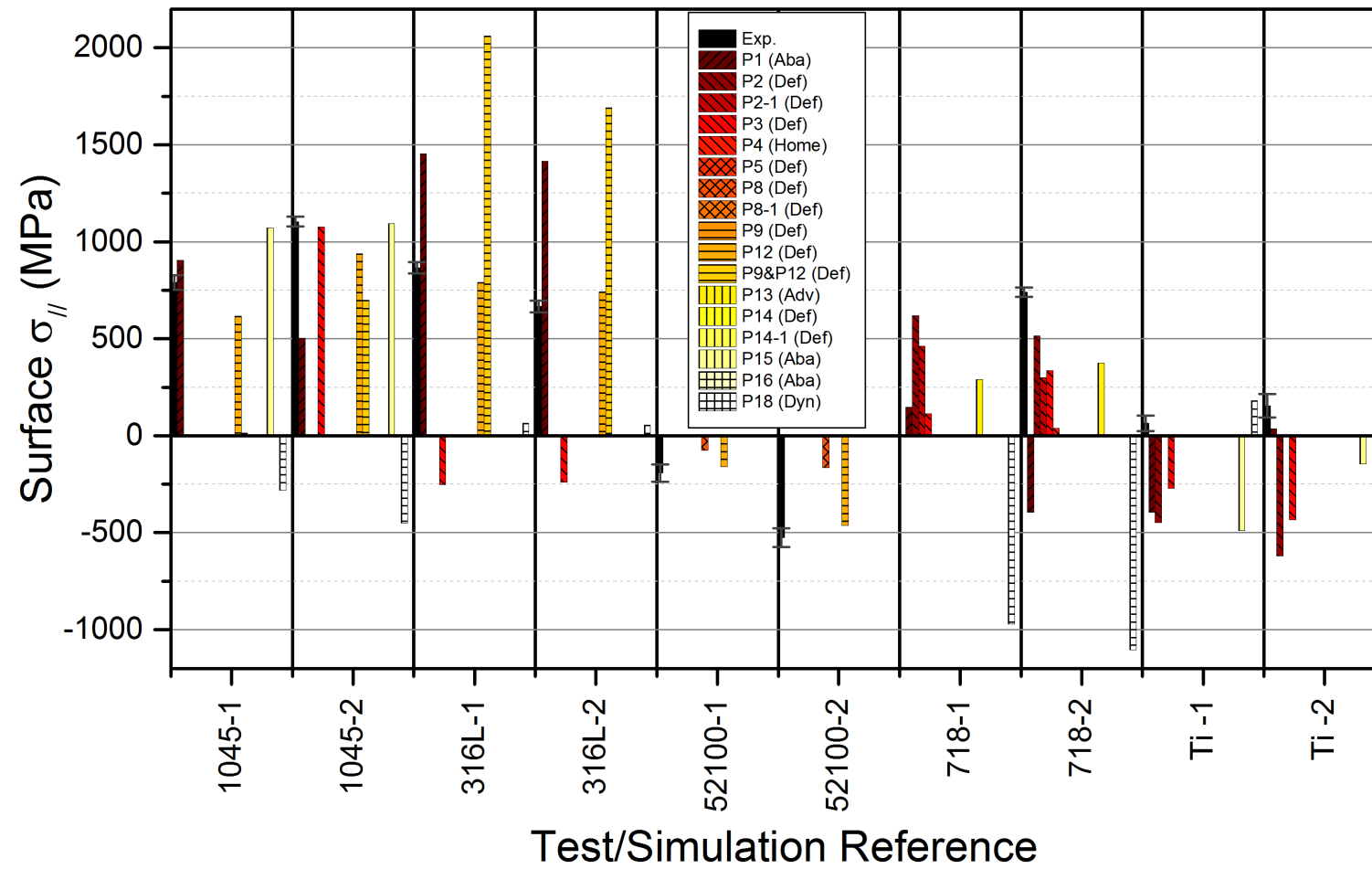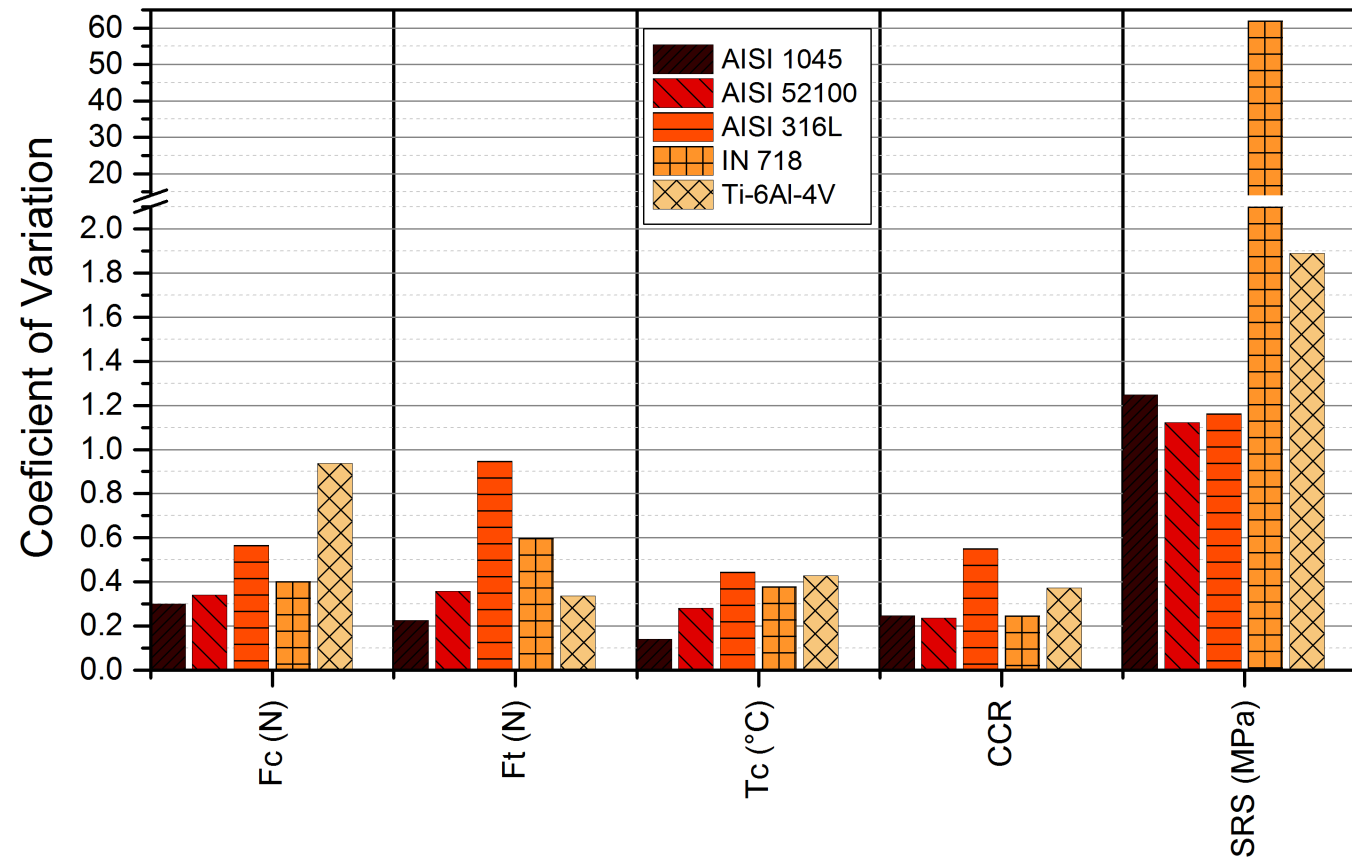
Figure 6. Simulated (color bars) and measured (black bar) Chip Compression Ratio (CCR), for different work materials and cutting conditions.

Figure 7. Simulated (color bars) and measured (black bar) surface residual stress σ//, for different work materials and cutting conditions.

Figure 8. Dispersion of the simulated results of cutting force, cutting temperature, CCR and surface residual stress (SRS) acting in the circumferential direction (σ//).
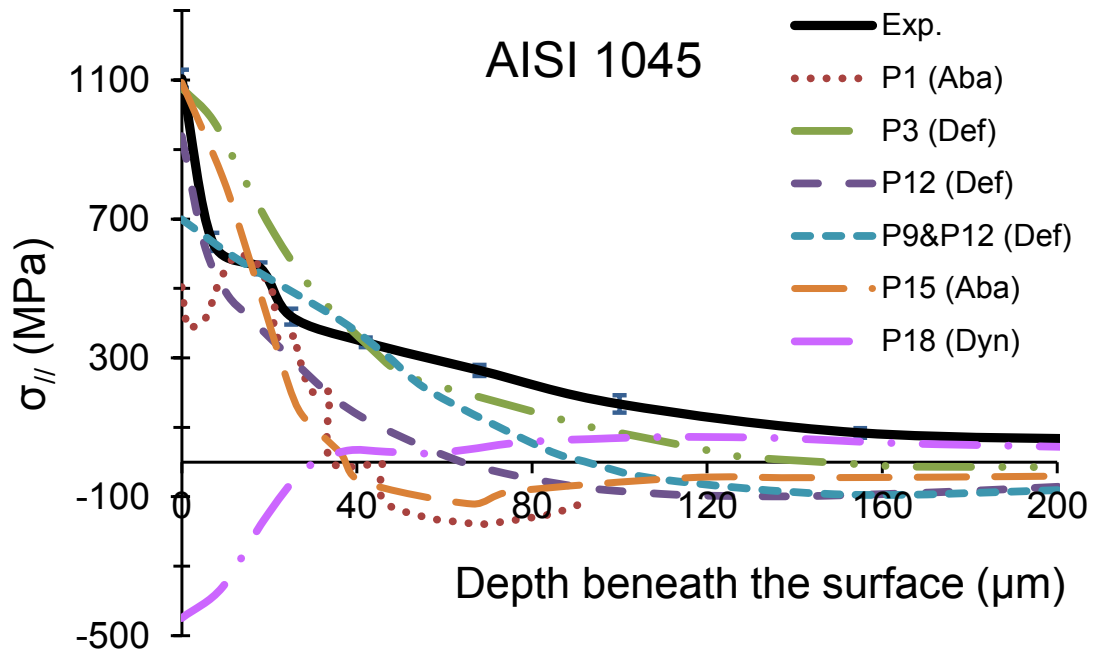
Figure 9. Simulated (color lines) and measured (black line) in-depth residual stress σ// profiles for the *AISI 1045* steel.
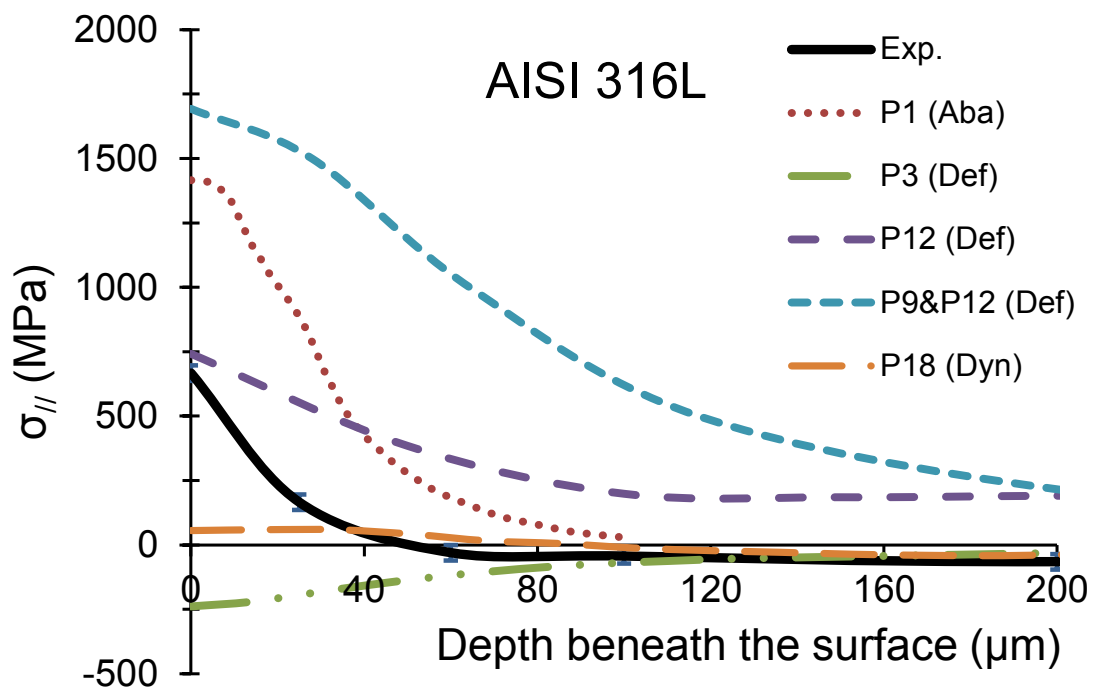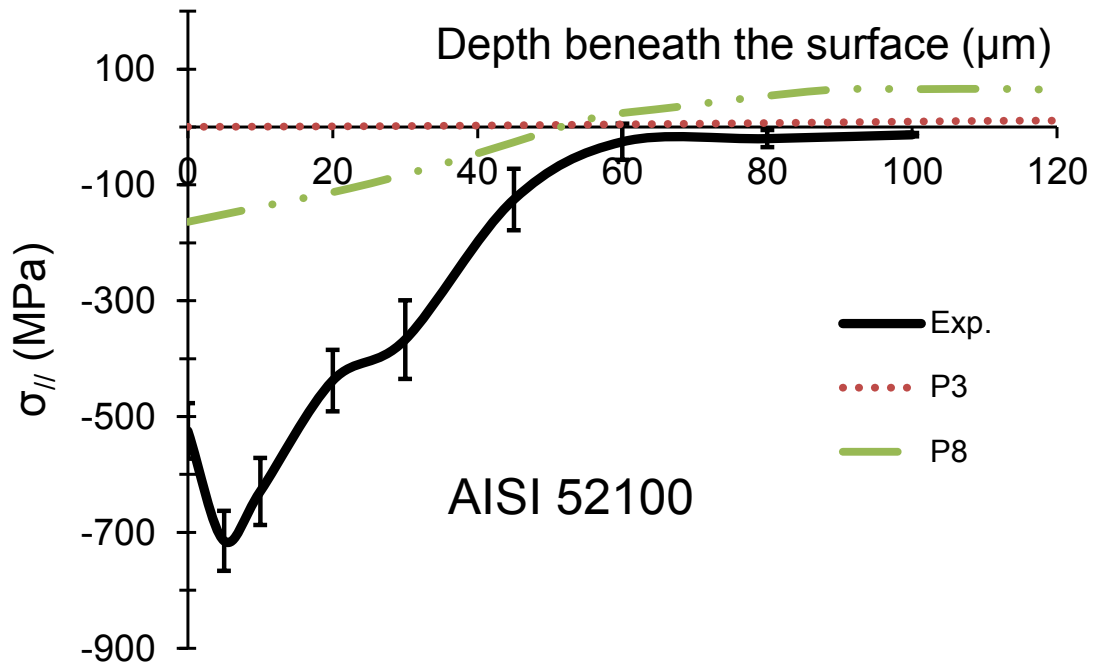

Figure 10. Simulated (color lines) and measured (black line) in-depth residual stress σ// profiles for the *AISI 316L* stainless steel.

Figure 11. Simulated (color lines) and measured (black line) in-depth residual stress σ// profiles for the *AISI 52100* hardened steel (Jawahir et al., 2011).
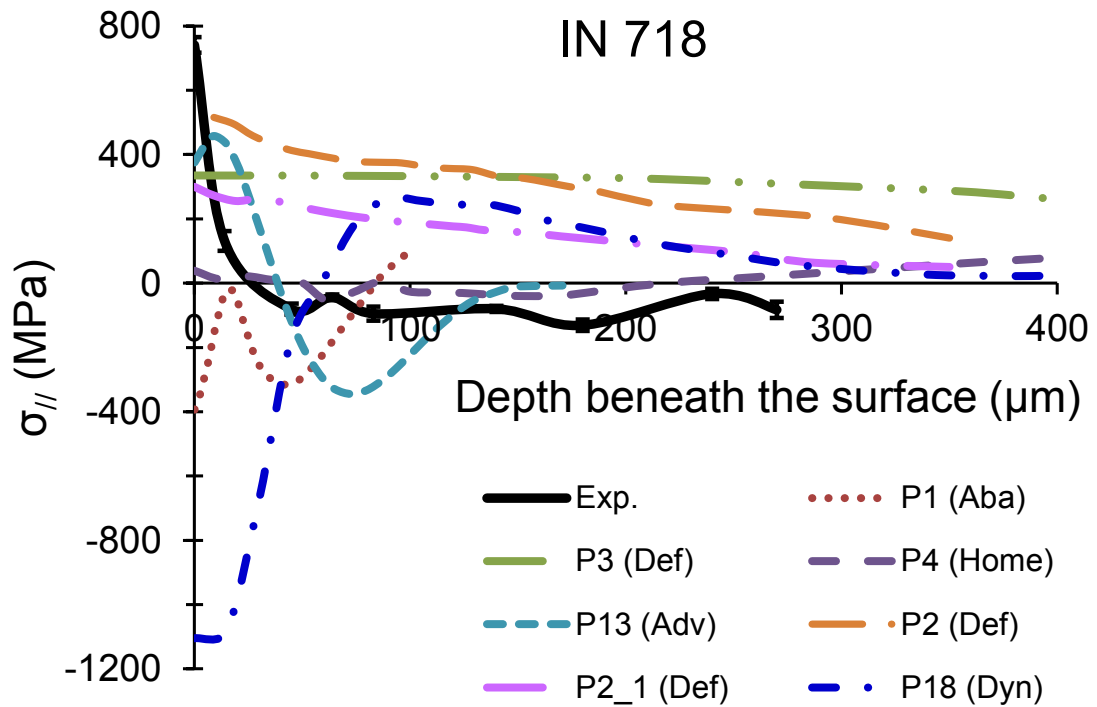

Figure 12. Simulated (color lines) and measured (black line) in-depth residual stress σ// profiles for the *Inconel 718* superalloy.
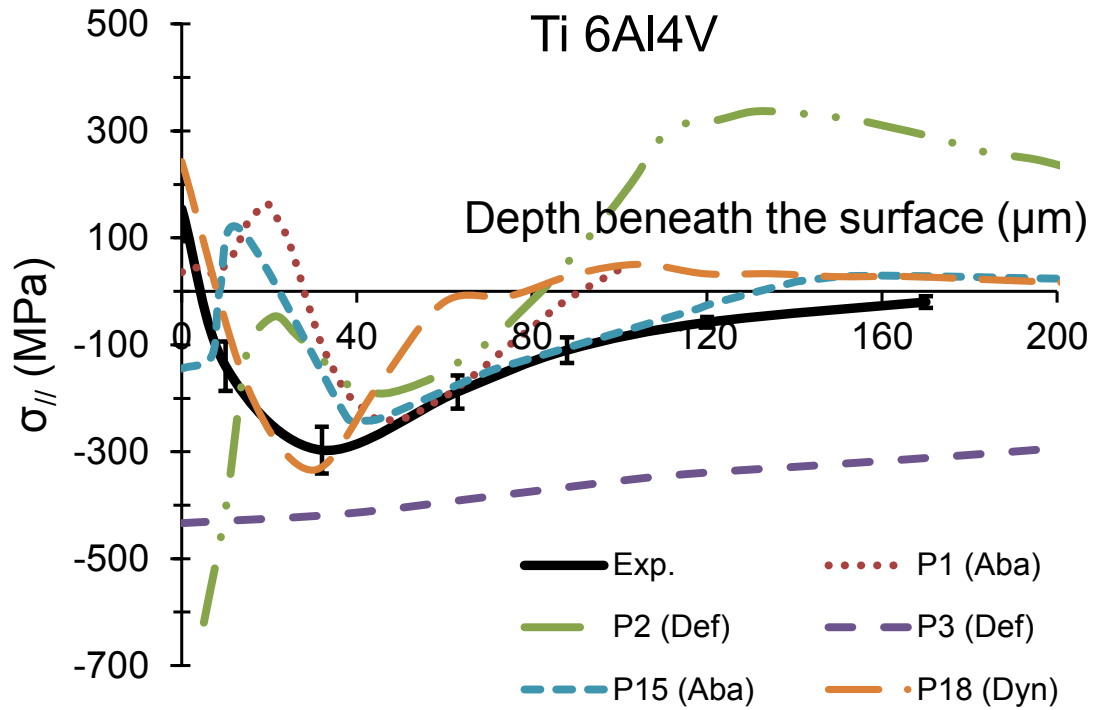
Figure 13. Simulated (color lines) and measured (black line) in-depth residual stress σ// profiles for the titanium *Ti6Al4V* superalloy.
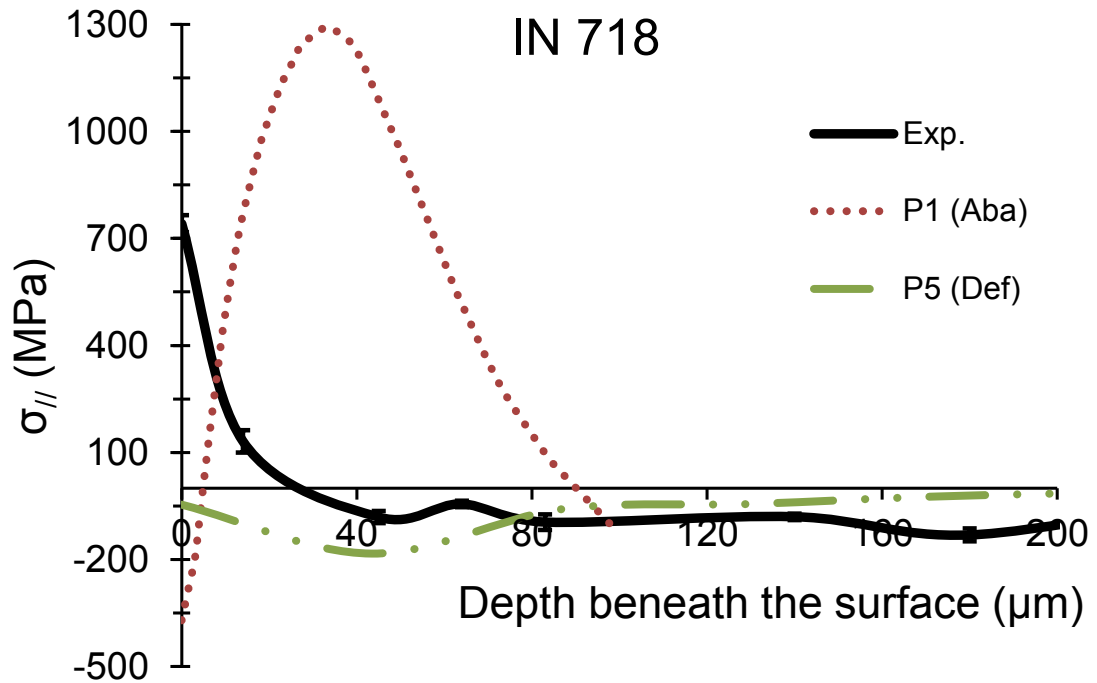

Figure 14. Simulated (color lines) and measured (black line) in-depth residual stress σ// profiles, after applying the calibration procedure (*Inconel 718)*.
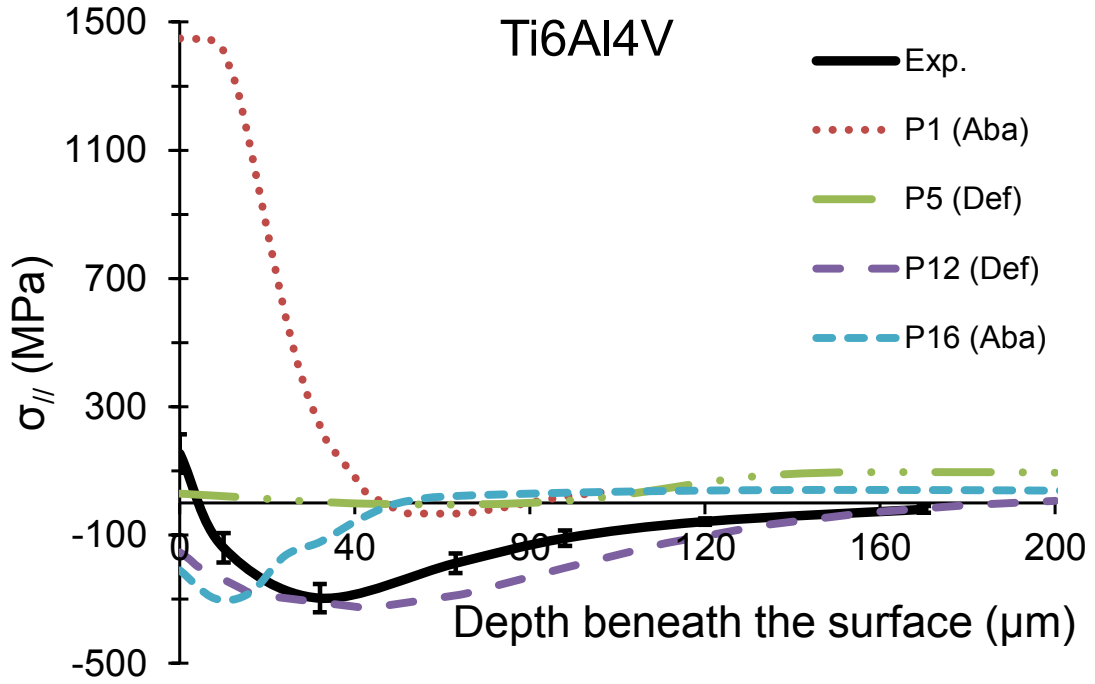
Figure 15. Simulated (color lines) and measured (black line) in-depth residual stress σ// profiles, after applying the calibration procedure (*Ti6Al4V*) (Jawahir et al., 2011).

CONCLUSIONS AND OUTLOOK

A benchmark study to evaluate the effectiveness of the current predictive numerical models for machining performance was conducted. This study included collaboration of 22 international participants from universities, research institutes and companies and/or software developers from 10 countries. Orthogonal cutting models of five work materials (*AISI 1045, AISI 52100, AISI 316L, IN 718* and *Ti-6Al-4V*) were developed and simulated using different commercial and non-commercial software packages (Ansys, Deform, LS-Dyna, AdvantEdge and a non-commercial software from the Yokohama National University), applying different numerical methods (FEM and Mesh-less) and formulations (Lagrangian, ALE). Predicted results (cutting and thrust

forces, cutting temperatures, chip compression ratio and residual stresses) obtained from different participants were compared with those results obtained experimentally. The results clearly show a high dispersion among the simulated results, with the dispersion higher for the residual stresses and lower for the chip compression ratio. Moreover, a higher dispersion of the results is generated for *AISI 316L, IN 718* and *Ti-6Al-4V* work materials when compared with *AISI 52100* and *AISI 1045* work materials. Concerning the comparison between predicted and measured results, the best predictions were obtained for *AISI 1045*, intermediate for *AISI 52100* and *Ti-6Al-4V* work materials, and the worst for *AISI 316L* and *IN 718* work materials. Thus, in general, the best uniformity among all predicted results and the best predictability were obtained for the *AISI 1045* work material.

Several factors will justify the obtained results, including the tool-chip contact and material constitutive models (including damage and fracture). Therefore, in order to improve the predictability of present metal cutting models, a proper selection of the tool-chip contact and material constitutive models, and the corresponding determination of their coefficients using well-designed experimental tests, is essential. Proper design of such experimental tests, and a careful analysis to the state of stress in the deformation zone would be required. This requires a complete overhaul of the classical metal cutting theories to accommodate more realistic observations in metal cutting.

ACKNOWLEDGMENTS

experimental tests: Dr. C. Fischer, Scientific Forming Technologies Corp. (SFTC), USA; Dr. R. Ivester, National Institute of Standards and Technology (NIST), USA; Dr. S. Rizzuti, Politecnico di Torino, IT; Prof. A. Del Prete, University of Salento, IT; Dr. N. Gramegna, Enginsoft, IT; Prof. D. Biermann and Prof. B. Svendson, University of Dortmund, DE; Prof. E. Ceretti, University of Brescia, IT; Prof. C. Giardini, University di Bergamo, IT; Prof. J. Rech, Ecole Nationale d'Ingénieurs de Saint-Etienne (ENISE), FR; Prof. J. Shinozuka, Yokohama National University, JP; Prof. M. H. Attia, McGill University, CA; Prof. J.P. Arrazola, University of Mondragon, SP; Prof. T. Ozel, Rutgers University, USA; Prof. Y. Karpat, Bilkent University, TR; Prof. V. Schulze, Karlsruher Institut für Technologie (KIT), DE; Prof. T. Mabrouki and Dr. Y. Zhang, INSA-Lyon, FR; Prof. K. Wegener, Dr. M. Röthlin, Dr. N. Rüttimann, IWF- ETH Zurich, CH.

REFERENCES

Abushawashi, Y.; Xiao, X.; Astakhov, V. (2011). FEM Simulation of Metal Cutting Using a New Approach to Model Chip Formation. International Journal of Advances in Machining and Forming Operations, 3: 71–92.

Abushawashi, Y.; Xiao, X.; Astakhov, V. (2013). A novel approach for determining material constitutive parameters for a wide range of triaxiality under plane strain loading conditions. International Journal of Mechanical Sciences, 74: 133–142.

Altintaş, Y.; Budak, E. (1995). Analytical Prediction of Stability Lobes in Milling. CIRP Annals - Manufacturing Technology, 44: 357–362.

Astakhov, V.P. (2006). Tribology of Metal Cutting, Elsevier: London.

Astakhov, V.P.; Outeiro, J.C. (2008). Metal Cutting Mechanics, Finite Element Modelling, in: Davim, J.P. (Editor), Machining: Fundamentals and Recent Advances. Springer.

Astakhov, V.P.; Shvets, S. (2004). The Assessment of Plastic Deformation in Metal Cutting. Journal of Materials Processing Technology, 146: 193–202.

Bai, Y.; Wierzbicki, T. (2008). A new model of metal plasticity and fracture with pressure and Lode dependence. International Journal of Plasticity, 24: 1071–1096.

Cockroft, M.G.; Latham, D.J. (1968). Ductility and Workability of Metals. Journal of the Institute of Metals, 96: 33–39.

Guo, Y.B.; Liu, C.R. (2002). FEM Analysis of Mechanical State on Sequentially Machined Surfaces. Machining Science and Technology, 6: 21–41.

Guo, Y.B.; Wen, Q.; Horstemeyer, M.F. (2005). An internal state variable plasticity-based approach to determine dynamic loading history effects on material property in manufacturing processes. International Journal of Mechanical Sciences, 47: 1423–1441.

Huang, J.M.; Black, J.T. (1996). An Evaluation of Chip Separation Criteria for the FEM Simulation of Machining. Journal of Manufacturing Science and Engineering, 118: 545–554.

Jaspers, S. (1999). Metal Cutting Mechanics and Material Behaviour (Ph.D), Technische Universiteit Eindhoven.

Jawahir, I.S.; Brinksmeier, E.; M'Saoubi, R.; Aspinwall, D.K.; Outeiro, J.C.; Meyer, D.; Umbrello, D.; Jayal, A.D. (2011). Surface integrity in material removal processes: Recent advances. CIRP Annals - Manufacturing Technology, 60: 603–626.

Johnson, G.R.; Cook, W.H. (1983). A Constuctive Model and Data for Metals Subjected to Large Strains, High Strain Rates and High Temperatures. Presented at the Proceedings of the 7th International Symposium on Ballistics, pp. 541–547.

Kolsky, H. (1949). An investigation of the material properties of materials at very high rates of loading. Proc Phy Soc B: Atomic and Molecular Physics, 62: 676–700.

Liu, M.; Takagi, J.; Tsukuda, A. (2004). Effect of tool nose radius and tool wear on residual stress distribution in hard turning of bearing steel. Journal of Materials Processing Technology, 150: 234–241.

M'Saoubi, R.; Outeiro, J.C.; Inal, K.; Lebrun, J.L.; Dias, A.M. (1997). Residual Stress and Texture Analysis in Machined Surfaces of AISI 316L Steels, in: al, E. by T.E. et (Editor), Presented at the Proceedings of The Fifth International Conference on Residual Stresses - ICRS5, pp. 349–354.

Mabrouki, T.; Girardin, F.; Asad, M.; Rigal, J.-F. (2008). Numerical and experimental study of dry cutting for an aeronautic aluminium alloy (A2024-T351). International Journal of Machine Tools and Manufacture, 48: 1187–1197.

Marques, M.J.; Outeiro, J.C.; Dias, A.M.; M'Saoubi, R.; Chandrasekaran, H. (2006). Surface Integraty of H13 ERS Mould Steel Milled by Carbide and CBN Tools. Materials Science Forum, 514-516: 564–568.

Movahhedy, M.; Gadala, M.S.; Altintas, Y. (2000). Simulation of the Orthogonal Metal Cutting Process Using an Arbitrary Lagrangian-Eulerian Finite-Element Method. Journal of Materials Processing Technology, 103: 267–275.

Outeiro, J.C.; Ee, K.C.; Dillon Jr., O.W.; Wanigarathne, P.C.; Jawahir, I.S. (2006a). Some observations on comparing the modelled and measured residual stresses

on the machined surface induced by orthogonal cutting of AISI 316L steel, in: I. Grabec, E.G. (Editor), Presented at the 9th CIRP International Workshop on Modeling of Machining Operations, University of Ljubljana, Faculty of Mechanical Engineering, pp. 475–481.

Outeiro, J.C.; Kandibanda, R.; Pina, J.C.; Dillon Jr., O.W.; Jawahir, I.S. (2010). Size-Effects and Surface Integrity in Machining and their Influence on Product Sustainability. International Journal of Sustainable Manufacturing, 2: 112 – 126.

Outeiro, J.C.; Rossi, F.; Fromentin, G.; Poulachon, G.; Germain, G.; Batista, A.C. (2013). Process Mechanics and Surface Integrity Induced by Dry and Cryogenic Machining of AZ31B-O Magnesium Alloy. Procedia CIRP, 8: 487–492.

Outeiro, J.C.; Umbrello, D.; M'Saoubi, R. (13). Experimental and FEM Analysis of Cutting Sequence on Residual Stresses in Machined Layers of AISI 316L Steel, in: Quander, W.R. and S. (Editor), Presented at the 7th European Conference on Residual Stresses (ECRS7), Published at Materials Science Forum - Trans Tech Publications, pp. 179–184.

Outeiro, J.C.; Umbrello, D.; M'Saoubi, R. (2006b). Experimental and numerical modelling of the residual stresses induced in orthogonal cutting of AISI 316L steel. International Journal of Machine Tools and Manufacture, 46: 1786–1794.

Özel, T.; Ulutan, D. (2012). Prediction of machining induced residual stresses in turning of titanium and nickel based alloys with experiments and finite element simulations. CIRP Annals - Manufacturing Technology, 61: 547–550.

Rech, J.; Arrazola, P.J.; Claudin, C.; Courbon, C.; Pusavec, F.; Kopac, J. (2013).

Characterisation of friction and heat partition coefficients at the tool-work material interface in cutting. CIRP Annals - Manufacturing Technology, 62: 79–82.

Rice, J.R.; Tracey, D.M. (1969). On the ductile enlargement of voids in triaxial stress fields. Journal of the Mechanics and Physics of Solids, 17: 201–217.

Silva, C.M.A.; Rosa, P. a. R.; Martins, P. a. F. (2012). Electromagnetic Cam Driven Compression Testing Equipment. Experimental Mechanics, 52: 1211–1222.

Umbrello, D.; Outeiro, J.C.; M'Saoubi, R. (2007). The Influence of Johnson - Cook Material Constants on Finite Element Simulation of Machining of AISI 316L Steel. International Journal of Machine Tools and Manufacture, 47: 462–470.

Umbrello, D.; Outeiro, J.C.; M'Saoubi, R.; Jayal, A.; Jawahir, I.S. (2010a). A numerical model incorporating the microstructure alteration for predicting residual stresses in hard machining of AISI 52100 steel. CIRP Annals - Manufacturing Technology, 59/1: 113–116.

Umbrello, D.; Outeiro, J.C.; M'Saoubi, R.; Jayal, A.D.; Jawahir, I.S. (2010b). A numerical model incorporating the microstructure alteration for predicting residual stresses in hard machining of AISI 52100 steel. CIRP Annals - Manufacturing Technology, 59: 113–116.

Valiorgue, F.; Rech, J.; Hamdi, H.; Gilles, P.; Bergheau, J.M. (2007). A new approach for the modelling of residual stresses induced by turning of 316L. Journal of Materials Processing Technology, 191: 270–273.